J Mater Sci (2007) 42:2820–2829
DOI 10.1007/s10853-006-1351-6

# Fracture behavior of notched specimens of TiAl alloys

J. H. Chen · R. Cao · J. Zhang · G. Z. Wang

Received: 28 July 2005 / Accepted: 28 February 2006 / Published online: 13 January 2007


**Abstract** Fracture behavior of a two-phase TiAl alloy was investigated using notched specimens. Fracture surfaces and metallographic sections of surviving notch in double notched specimens are observed. The fracture process of notched specimens of TiAl alloys was described as that several inter-lamellar cracks initiate and extend directly from the notch root and propagate preferentially along the interfaces between lamellae and stop at various obstacles. With increasing applied load, cracks connect with each other and propagate further by translamellar cracks. The toughening mechanisms, which make the main crack difficult to propagate or cause it to be stopped, could be reducing the driving force for crack propagation. The higher toughness of near fully lamellar microstructure than that of finer duplex microstructure is attributed to the path of crack propagation. On the fracture surfaces of the finer duplex microstructure, more low-energy-spending interlamellar fracture facets are observed, which means that it is easier for crack to bypass a fine duplex lamellar grain with lamellae perpendicular to the main crack and to take a interlamellar path.

J. H. Chen (✉) · R. Cao · G. Z. Wang
State Key Laboratory of Gansu Advanced Non-ferrous Metal Materials, Lanzhou University of Technology, Lanzhou, Gansu 730050, China
e-mail: zchen@lut.cn

J. Zhang
High Temperature Material Research Division, Central Iron and Steel Research Institute, Beijing 100081, China

## Introduction

Considerable interest exists in the development of titanium aluminide (TiAl) alloys for use in high-temperature structural applications, due to their low density, strength retention at high temperature, and potential for excellent fatigue resistance [1–4]. Much research work has been done on the fracture processes and toughening mechanisms of TiAl alloys [4–12]. Chan et al. [6] have shown that the initiation of micro-cracks either at colony boundaries, along lamellar interfaces, or at equiaxed $\gamma$ grains located at colony boundaries and the linkage of the micro-cracks with the main crack by shear fracture of the near-tip ligaments dominate the fracture process in the lamellar microstructure. Lu et al. [7] and Inui et al. [12] indicated that the crack propagates either along lamellar interfaces (interlamellar fracture) or skews to the lamellae (translamellar fracture), depending on the direction of the main crack relative to the lamellae.

Recently, Chan et al. [8] examined cracking of polycrystalline lamellar Ti–46.5%Al compact-tension specimens in situ in the scanning electron microscopy (SEM). They reported a low initiation toughness value in the range of 1.2–4 $\mathrm{MPam}^{1/2}$, predominantly interlamellar cracking within the colony with crack advancing by the linking up of a minimal number of small microcracks ahead of the main crack, negligible resistance to crack growth within certain colony, and noticeable resistance to crack growth across colony boundaries. They further showed that the magnitude of the resistance to crack growth offered by the boundaries was dependent on the lamellar misorientation across the boundaries. However, in the [13], they have demonstrated that the preferred fracture mode within a colony is delamination along $\gamma/\alpha_2$ interfaces and or within $\alpha_2$ lamellae and that this occurs with virtually no resistance ($K_{eq}$ = 0.6–1.8 MPam$^{1/2}$). But colony boundaries were effective in stopping an advancing crack if the lamellar twist misorientation across the boundaries is large, a boundary resistance to crack growth could be clearly measured in such a situation.

Guo et al. [14] studied the effect of internal stress on the fracture toughness of a TiAl-based alloy with duplex microstructure. It was found that internal stress play an important role in determining the fracture toughness of the TiAl-based alloy, the compression internal stresses in $\gamma$ phase and the tensile internal stresses in $\alpha_2$ phase may be responsible for the delamination along the $\gamma/\alpha_2$ boundaries. In our previous work [15] by in-situ observation of surface fracture process of very thin specimens, the present authors indicated that: cracks prefer to initiate and propagate along lamellar interfaces, which are the weakest link in the near fully lamellar microstructure. The interlamellar strength is significantly lower than the translamellar strength. The tensile stress is the driving force for crack initiation and propagation. The main crack stops in front of grains having lamellar interfaces perpendicular to or inclined with a large angle to the direction of propagation, and new cracks are nucleated at lamellar interfaces behind the barrier grain. The main crack and new cracks are linked by the translamellar cleavage fracture of the barrier grain with increasing applied load. In work [5], the present author found that the cracks extended directly from the pre-crack tip and are triggered and driven by tensile stress.

In this work, the authors examine further the fracture process and the toughening mechanism of a two-phase TiAl alloy with notched block specimens carefully.

## Experimental

### Materials and specimens

A nominal chemical composition of the material used in this study was shown in Table 1**,** all the compositions in this paper are given in atom percentage. Two types of microstructures, duplex (DP) and near fully lamellar (NFL) were prepared. All samples were taken from a forged pancake that had been deformed at 1100 °C for 50% height reduction. Annealing at 1290 °C for 6 h followed by a stabilizing treatment at 950 °C for 12 h was employed to produce the DP microstructure. For the NFL microstructure, the samples were first annealed at 1100 °C for 36 h, reheated to 1360 °C for 12 min and then stabilized at 950 °C for 12 h. The samples were enclosed in quartz tubes and put into the furnace at the determined temperatures. The cooling rate from the alpha field was around 20 °C per minute. It was found that after stabilizing the cooling rate had no significant influence on the lamellar space. The alpha transformation temperature is 1365 °C. The DP microstructure is shown in Fig. 1(a) as 160 μm $\gamma/\alpha_2$ lamellar grains with $\gamma$ grains at the boundaries. The NFL microstructure is shown in Fig. 1(b) as elongated $\gamma/\alpha_2$ lamellar grains with the size of around 80 × 320 μm.

The dimensions of the flat tensile specimen are shown in Fig. 2(a), the dimensions of the cubic compression specimen are shown in Fig. 2(b), and all specimens were polished before testing. The dimensions of four point bending (4PB) specimens with and without a notch are shown in Fig. 3(a), (b) and (c). For doubly notched specimens, fracture occurred at one notch, the critical condition was reached in the vicinity of the surviving notch denoting the other notch, which had not been fractured. Double notched specimens were prepared for observing remaining crack on the metallographic sections perpendicular to the surviving notch root after the specimen was fractured at one notch. Specimens without notch were prepared for comparing and investigating the effect of the notch.

**Table 1** Compositions of TiAl alloy (at %)

| Ti | Al | V | Cr | Ni | B | O |
|---|---|---|---|---|---|---|
| Balance | 46.3 | 2.0 | 1.0 | 0.5 | 0.1 | 0.07 |

### Mechanical tests

Tensile and compression tests were conducted in air at room temperature by a SHIMADZU AG-10TA universal test machine with a cross head speed of 0.025 mm/min. The yield stress ($\sigma_{0.2}$), ultimate tensile strength ($\sigma_{uts}$), total elongation (fracture strain $\varepsilon_f$), fracture stress ($\sigma_f$) and elastic modulus ($E$) were measured from engineering stress–strain curves of both tensile and compression tests [15]. All values of stress are defined as the corresponding loads divided by the original section areas. The strain within the gauge length of the specimen is measured by an extensometer.

4PB tests were carried out in air at room temperature by a SHIMADZU AG-10TA universal test machine with a cross head speed of 0.5 mm/min. The fracture load $P_f$ was measured directly from the

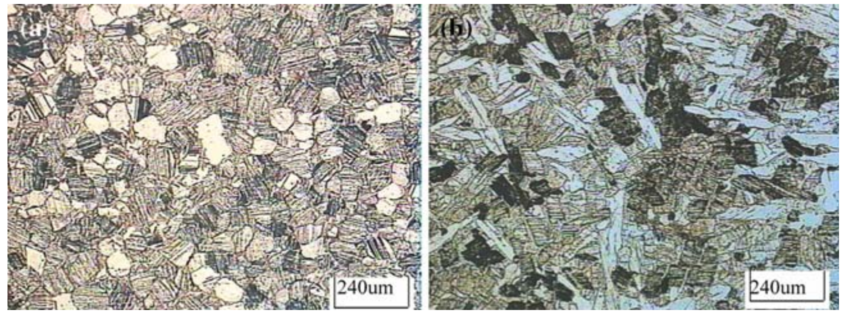


**Fig. 1** Microstructures of (**a**) Duplex (**b**) Near fully-lamellar TiAl alloy

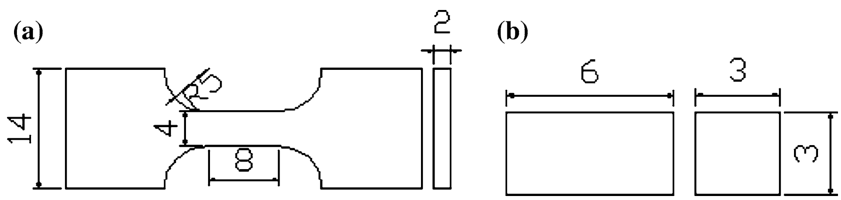


**Fig. 2** Dimensions of specimens for (**a**) Flat tensile tests (**b**) compression tests

load–displacement curve, and the energy absorbed in fracture was measured by the area under the load–displacement curve.

## Fracture surface observations

Fracture surface observations were carried out on all fractured specimens by SEM. Besides the general pattern of whole fracture surface, attention was focused on the region around the notch root to find out if cracks were initiated in front of the notch root or were just extended directly from the notch root.

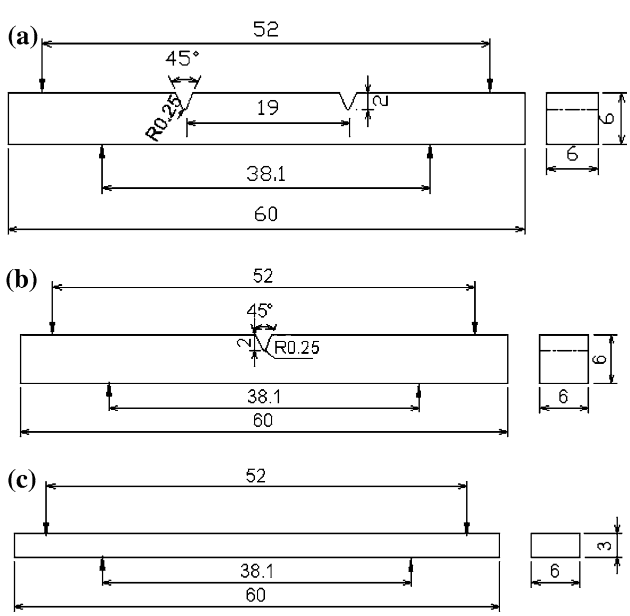


**Fig. 3** Dimensions of four point bending (4PB) specimens (**a**) with double notch, (**b**) with single notch, (**c**) without notch

## Observations of metallographic sections

Five metallographic sections were cut perpendicular to the surviving notch root after the specimen was fractured at a notch. The path of remaining cracks on the polished and etched metallographic section can be followed by SEM observation to investigate the fracture behavior in details.

# Experimental results

## Macroscopic mechanical tests

Results of tensile tests are provided in [15]. The stress–strain curves obtained from tensile and compression tests of the specimens with DP and NFL microstructures are plotted in Fig. 4.

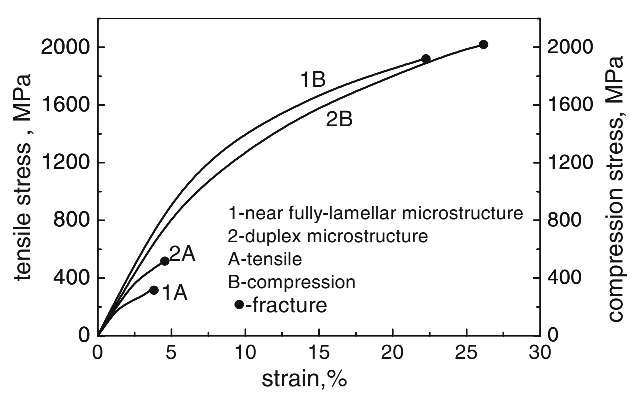


**Fig. 4** Engineering stress–strain curves of tensile and compressive tests of near fully lamellar and duplex TiAl alloys

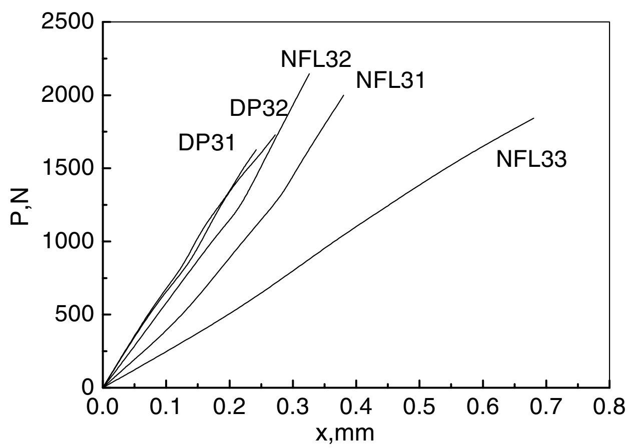


**Fig. 5** Load–displacement curves obtained from 4PB tests of the specimens with the two microstructures

The load–displacement curves obtained from 4PB tests of the specimens with DP and NFL microstructures are plotted in Fig. 5. The measured macroscopic mechanical parameters and dimensional parameters are listed in Table 2.

The remarkable differences between results of tensile tests and compression tests were explained in [15]. From Table 2, it is found that the values of fracture energy absorbed in both single and double notched specimens for coarser near fully lamella microstructure are higher than for finer duplex microstructure, even though the later shows superior tensile strength and ductility as shown in Fig. 4. It means that the inverse ductility/$K_{1C}$ relationships presenting in precracked specimens [2] also present in notched specimens.

## Fracture surface observation

A general cleavage pattern is shown in fracture surface for all specimens. Figure 6 shows three typical regions ahead of the fracturing notch root of a single notched NFL specimen. Most cracks initiate and extend directly from the notch root. Only one crack (marked by a black arrow in Fig. 6(c)) initiates at a distance of 40 $\mu$m from the root.

In Fig. 7(a), three regions on the fracture surface of a single notched DP specimen also show interlamellar cracks initiating and extending directly from the notch root and separated by translamellar cracks. Several cracks can be initiated at points inside the ligament (shown by arrows in Fig. 7(b), (c)), but never a crack initiation center, which triggers the cleavage and makes the catastrophic fracture of whole specimen as observed in HSLA steels be found.

Figure 8 shows the typical fracture surfaces of double notched specimens of both NFL and DP microstructures. As the same as observed in single notched specimens, cracks initiate at the notch root and extend directly from the notch root. In NFL specimens, elongated interlamellar fracture facets are dominant (Fig. 8a)). However, in DP specimens, square interlamellar fracture facets dominate (Fig. 8(b)). This phenomenon is consistent with the micro-structural characteristic shown in Fig. 1 where NFL microstructure shows elongated $\gamma/\alpha_2$ lamellar grains however DP microstructure shows equiaxed lamellar grains. It is worth noting that more potions of interlamellar fracture facets are observed on fracture surfaces of specimens of DP microstructure than that of specimens of NFL microstructure.

Figure 9 shows the fracture surfaces of specimen of NFL microstructure without notch. The general pattern is similar to that of notched specimen. Cracks extend directly from the tensile-stressed side.

## Observation of metallographic section

Figure 10 shows 5 metallographic sections of the surviving notch root of a double notched DP specimen showing the remaining cracks. These cracks initiate and extend directly from the notch root and propagate preferably along interface between lamellae or grain boundaries. At the moment of fracturing of the other notch, the load is released suddenly, the crack stops and remains in the vicinity of the surviving notch root.

**Table 2** Results of 4PB tests at room temperature

| No | Notch type | $w$ (J) | $w'$ (J/mm$^2$) | $P_f$ (N) | $W$ (mm) | $B$ (mm) | $a$ (mm) |
|---|---|---|---|---|---|---|---|
| NFL31 | Single notch | 0.332 | $13.293 \times 10^{-3}$ | 1999.2 | 6.068 | 6.116 | 2 |
| NFL32 | Double notch | 0.321 | $12.179 \times 10^{-3}$ | 2146.2 | 6.141 | 6.292 | 2 |
| NFL33 | smooth | 0.626 | $33.389 \times 10^{-3}$ | 1842.4 | 6.115 | 3.066 | – |
| DP31 | Single notch | 0.199 | $7.804 \times 10^{-3}$ | 1528.8 | 6.134 | 6.157 | 2 |
| DP32 | Double notch | 0.243 | $9.554 \times 10^{-3}$ | 1728.7 | 6.142 | 6.141 | 2 |

No = specimen's number, NFL = near fully-lamellar, DP = Duplex, $P_f$ = fracture load, $w$ = energy absorbed in fracture, $w'$ = fracture energy by unit area, $W$ = specimen's width, $B$ = specimen's thickness, $a$: notch depth

**Fig. 6** Fracture surface of single notch specimen for near fully-lamellar microstructure (NFL31)

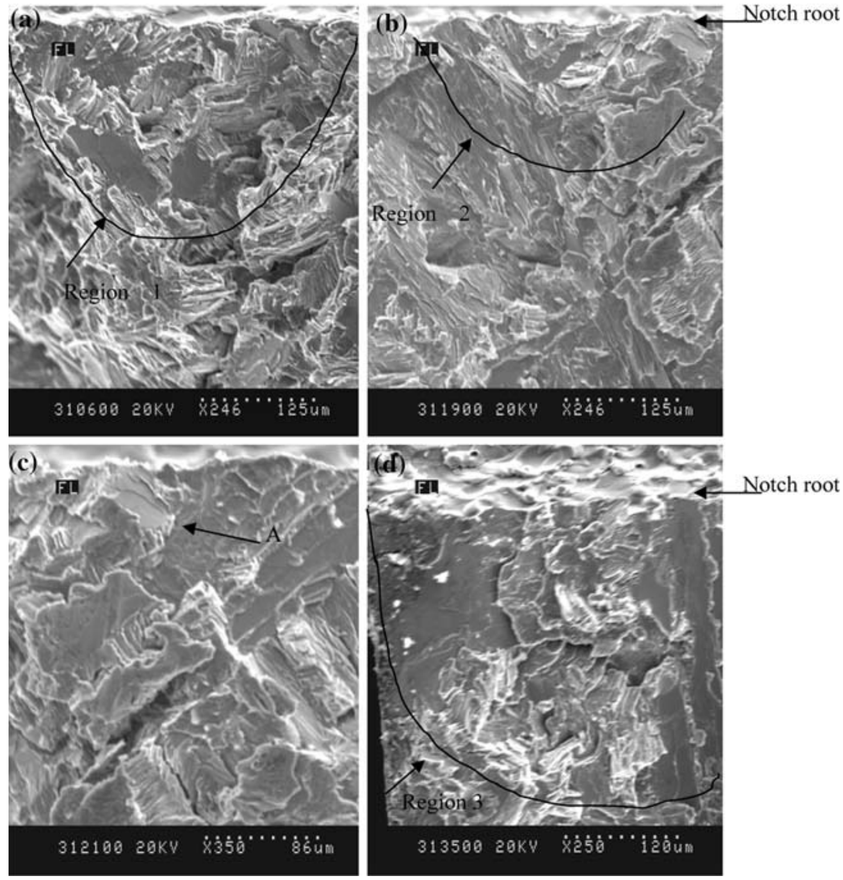


Figure 11 shows the vicinity of the root of the surviving notch in the metallographic sections of double notched NFL specimen. It is found that most grains around the surviving notch root show the lamellae with orientation unfavorable for cracking under the tensile stress action (shown by arrows in Fig. 11(a)). It may be the reason why there is no remaining crack, even in the very vicinity of the surviving notch root (shown by bracket 3 and 4).

## Discussion

### Process of fracture

From Figs. 6–8, it is observed that most cracks initiate and extend directly from the notch root for both NFL and DP single or double notched specimens. Although several cracks initiate at points a distance from the notch root, yet never a crack initiation center, which triggers the cleavage and makes the catastrophic fracture of whole specimen, can be found. It is very different from that observed in HSLA steels [16], where a cleavage crack always initiates at a distance from the notch and catastrophically propagates towards both the notch root and the rest ligament. Figure 10 of the metallographic sections supports above idea. The cracks prefer to extend directly from the surviving notch root and through the interlamellar layers or grain boundaries. Most cracks stop at or in front of a grain with orientation unfavorable to crack propagation, the tips of remaining crack are remarkably blunted. In specimen without notch, cracks initiate and extend from the tensile stressed site (Fig. 9), where the tensile stress is highest. The mechanism of crack initiation and propagation is similar to that the cracks initiate and extend from notch root for notched specimens.

In fact, in-situ tests are used to study the fracture process and fracture mechanisms, in-situ tensile tests are valuable to evaluate fracture process of tensile tests [8, 15], however, it is very difficult to study fracture process of bending tests. For doubly notched bending tests, fracture occurred at one notch and the critical condition was reached in the vicinity of the survived notch. Authors have done many studies about fracture mechanisms of HSLA steels by this methold [16]. Figures 10 and 11 are metallurgical

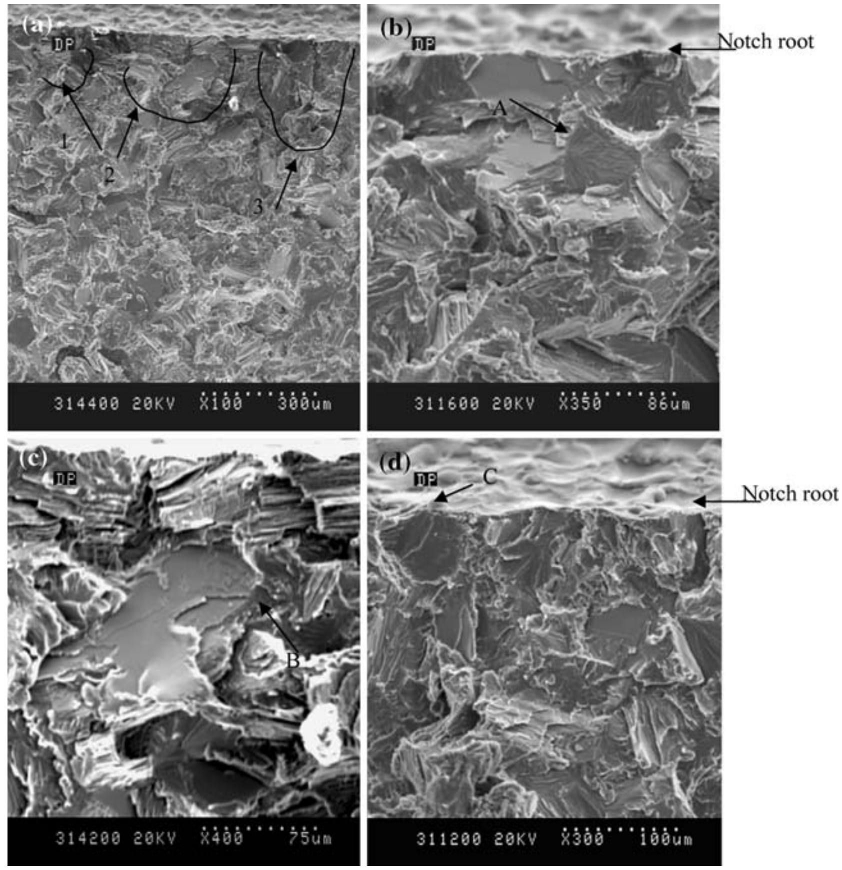


**Fig. 7** Fracture surface of single notch specimen for duplex microstructure (DP31)

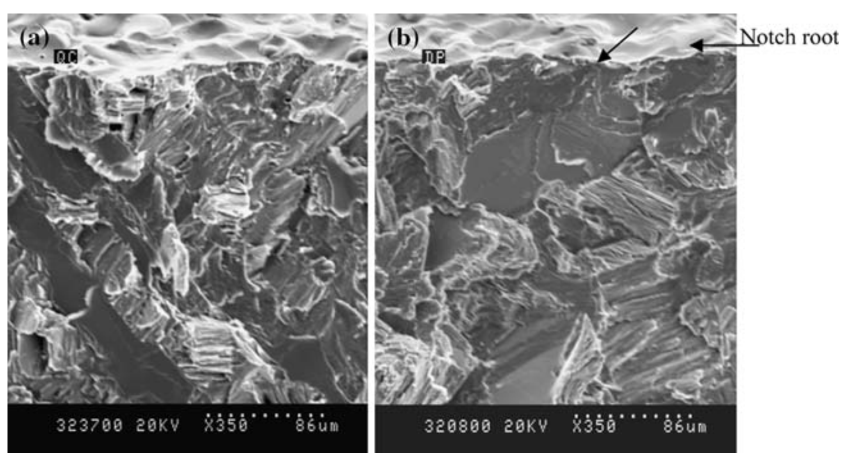


**Fig. 8** Fracture surface of double notch specimens (**a**) for near fully-lamellar microstructure (NFL32), (**b**) for duplex microstructure (DP32)

sections of surviving notches in DP and NFL specimens, From these figures, we could attain the following ideas: interlamellar cracks and cracks along grain boundary are found in the surviving notch root, so it is presumed that the fracture process of DP specimens is crack propagation-controlled process, i.e. Cracks are easy to produce, crack propagation are difficult, so more toughening phenomena appear. For NFL specimens, No cracks are found in the surviving notch root of NFL specimens in Fig. 11, i.e. no cracks are produced at the moment of fracture. It is attributed to that in this specimen the lamellar orientations of grains in front of notch tip are parallel to the principle stress and the translamellar strength is larger than interlamellar strength.

Based on Fig. 10, the cracks preferably initiate and propagate along interface between lamellae and stop at various obstacles, and in Figs. 6 and 7 the interlamellar crack facets are separated by translamellar crack facets. Combining the results obtained in work [15]

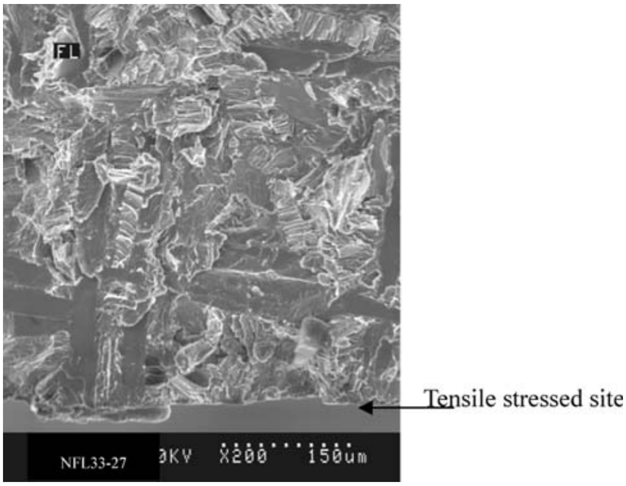


**Fig. 9** Fracture surface of specimen without notch for near fully-lamella microstructure (NFL33)

and [17], by in-situ tensile tests in SEM and by unloading of 3PB tests of precracked specimens, the present authors suggested the crack propagation in TiAl alloy is stress driven and forwards step by step. This is unlike in the HSLA steels where the cleavage crack initiates and catastrophically propagates through whole specimen. In this work, while the crack is short, the stress is controlled by the field established by the notch, with increasing the applied load, the stress at the hindered crack tip increases, the crack overcomes various obstacles extends further. Until the crack extends to an extent the stress at its tip is controlled by the produced crack configuration itself and keeps a higher lever, the crack extends unstably and causes the fracture of whole specimen.

There is no any trace of plastic deformation observed in microscopic scale. The feature of the fracture surface is of typical cleavage. No any tear ridge between fracture facets and stretch zone between notch root and cleavage crack are found. No cavity and slip lines are found in metallographic sections. Blunting of crack is caused by elastic damage than by plastic strain. The present authors cannot conclude that in a block specimen the cleavage cracks still initiate and propagate in a microscopically elastic environment, but from above phenomena the present authors can conclude that plastic strain is not to be of decisive role in cleavage crack initiation and propagation in TiAl alloys. So the driving force for crack initiation and propagation is the tensile stress.

## Toughening mechanism in the TiAl alloy

Figure 10 shows following agencies to reduce the driving force for crack extending:

(1) Blunting of crack tip: almost in all cases the crack tip is blunted to 4–6 $\mu$m in radius much larger than that in steel at low temperature.
(2) A bifurcation of crack branch as shown by Fig. 10(i), which disperses the tensile stress.
(3) The deflection of the main crack by the lamellae as shown by Fig. 10(a), (c), (d), (g).
(4) Formation of a diffuse zone of micro-cracks (Fig. 10(a), (g), (i), which reduces the stress triaxiality around the main crack.

Figure 10 also shows following barriers stopping the crack:

(1) Barrier made by a grain with a lamellar interface orientation unfavorable for crack propagation as shown in Fig. 10(d), (j), it is shown by black arrow 1 in these figures.
(2) Barrier made by grain boundary between lamellar grain and ( grains as shown by Fig. 10(b), (d), (f), (h), (j), it is shown by black arrow 2 in these figures.

Above agencies are considered as the main factors toughening the TiAl alloy.

In summary, almost all mechanisms are related to the lamellar structure, which could be thought of as a composite consisting layer by layer of more plastic $\gamma$ and of harder $\alpha_2$. The interlamellar strength is very low, but the translamellar strength is much higher than the interlamellar strength. The lamellar structure with different strength in trans- and inter-lamellar directions can deflect the crack, blunt its tip, cause bifurcation and produce a defused zone of microcracks. It is the reason why the fully lamellar structure is used in growth. But in our work, the shear-ligament toughening suggested by previous work [6–11] is not found.

## The inverse relationship between tensile strength (ductility) and notch toughness of finer duplex and coarser near fully lamella microstructures

The inverse ductility/$K_{1C}$ relationship is also observed in this work, finer DP microstructure shows higher tensile ductility in tensile tests [15], but lower fracture toughness (Table 2).

Comparing the fracture surface of notch specimens (Fig. 8), it is noted that in general more potions of interlamellar fracture facets are observed on fracture surfaces of finer duplex microstructure specimens than of coarser near fully lamellar microstructure specimens. It is reasonable to infer that it is easier for the crack to bypass a smaller grain with unfavorable orientation and find the interlamellar propagating path

**Fig. 10** Metallographic sections of the surviving notch of double notches specimen of duplex microstructure (DP32)

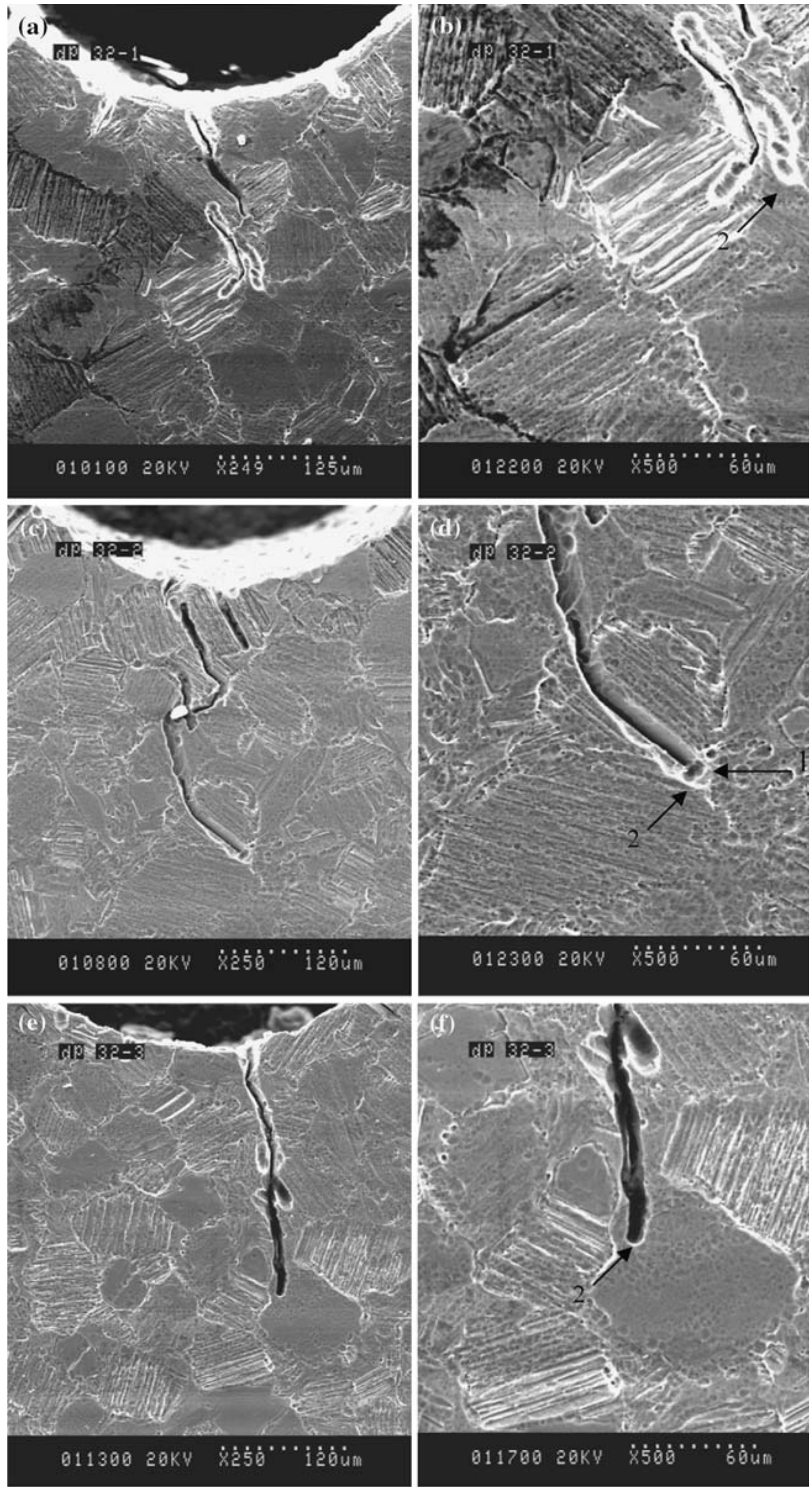


in the finer duplex microstructure than in the coarser near fully lamellar microstructure. It means that in coarser near fully lamellar microstructure, the crack should skew through larger grains with unfavorable orientation or bypass them by much more tortuous path and causes a much rough fracture surface. It is the reason why the coarser near fully lamellar microstructure shows high notch fracture toughness even though it has similar interlamellar strength to that of the finer duplex microstructure. But in the tensile test specimens

**Fig. 10** continued

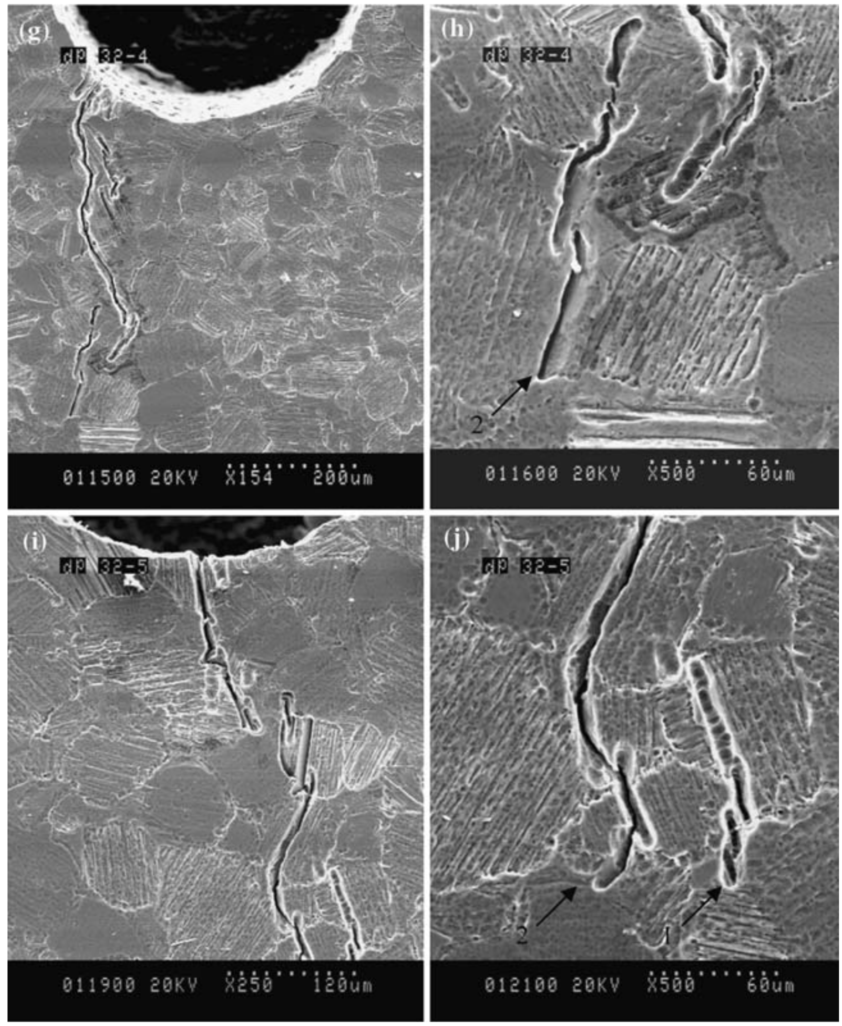


**Fig. 11** Metallographic sections of the surviving notch of double notches specimen of near fully-lamellar microstructure (NFL32)

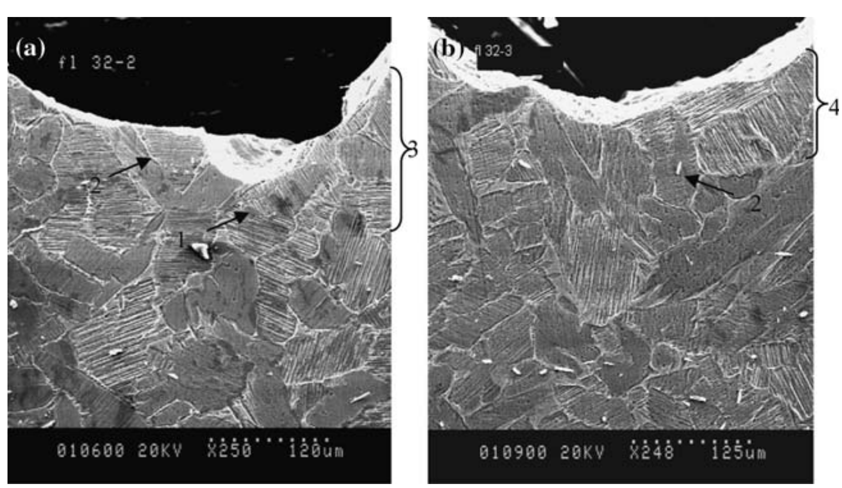


the sampling volume (which involves all volume within the gauge) are much larger than that in the notched specimens (restricted by the notch). It is reasonable to infer that for a smooth plan specimen for tensile test, more choices of lower resistance paths can be taken, where much larger sampling volume exists. Therefore in a tensile specimen the cleavage fracture is able to take the weakest way with highest portions of interlamellar cracking. The superiority of coarse lamellar grains shown in the notched specimen, where the sampling volume is seriously restricted, cannot act in effect.

For tensile test specimens of both microstructures, the cracks can propagate through the way with minimum resistance. In this case, the coarse grain microstructure shows lower resistance and causes a low strength and ductility.

### The effect of notch

The main effect of the notch presents in increasing the tensile stress at and ahead of the notch root and make it easy to initiate and propagate the crack. From Table 2, the energy absorbed by unit area of specimen with a notch or double notches is lower than that of specimen without a notch. The notch also establishes a higher stress triaxiality, which makes it possible to initiate a crack at a distance from the notch root.

The effect of notch presents until the crack reaches an extent then the stress will be controlled by the crack configuration itself.

## Conclusions

Combining macro experimental results of the 4PB tests, detailed observations of fracture surfaces and remaining cracks at the surviving notch root of a two phase TiAl alloy, following conclusions can be drawn:

1. The fracture process of notched specimens of TiAl alloys is follows: several inter-lamellar cracks initiate and extend directly from the notch root and propagates preferentially along the interfaces between lamellae and along grain boundaries, and stops at boundaries of grains with unfavorable orientations. The driving force for crack propagation is the tensile stress. With increasing the tensile stress, the crack extends further across the barrier grain.
2. The mechanism of toughening the TiAl alloys may be reducing the driving force by blunting of the crack tip, bifurcation of the crack tip, formation of defuse zone of microcracks, and deflection of the crack by lamellae and stopping the crack by the boundary of grain with unfavorable orientation or of grain $\gamma$.
3. The inverse relationship between tensile ductility and notch toughness of finer duplex and coarser near fully lamellar microstructures is caused by the different crack propagation path taken by the crack between the tensile test and the notch bending test due to the different sampling volume.

**Acknowledgements** This work was financially supported by the National Natural Science Foundation of China (No. 50471109), the National Natural Science Foundation of Gansu Province (No. 3ZS061-A25-037) and Opening Foundation of State Key Laboratory of Gansu Advanced Non-ferrous Metal Materials.

## References

1. Kim YW (1989) JOM 41(7):24
2. Kim YW (1991) JOM 43(8):40
3. Yamaguchi M, Inui H (1993) Structural intermetallics, TMS, Pittsburgh, PA, p 127
4. Kim YW (1994) JOM 46(7):30
5. Chen JH, Pippan R, Hebesberger T (2002) Int J Fracture 113:327
6. Chan KS, Kim YW (1992) Metall Trans A 30A:1663
7. Lu YH, Zhang YG, Chen CQ (1999) Gamma titanium aluminides, edited by Kim Y-W, Dimiduk DM, Loretto MH, Minerals, Metals and Materials Society, 595
8. Chan KS, Onstott J, Kumar KS (2000) Metall Trans A 31A:71
9. Arata JJM, Kumar KS, Curtin WA, Needleman A (2001) Int J Fracture 111:163
10. Chan KS (1993) Metall Trans A 24A:569
11. Kim YW, Dimiduk DM (1997) George Irwin R. Symposium on Cleavage Fracture, edited by Chan KS, The Minerals, Metals and Materials Society, 305
12. Inui H, Oh MH, Nakamura A, Yamaguchi M (1992) Acta Metall Mater 40:3095
13. Wang P, Bhate N, Chan KS, Kumar KS (2003) Acta Metall Mater 51:1573
14. Guo FA, Ji V, Francois M, Zhang YG (2003) Acta Mater 51:5349
15. Chen JH, Cao R, Wang GZ, Zhang J (2004) Metall Mater Trans A 35A:439
16. Chen JH, Wang Q, Wang GZ, Li Z (2003) Acta Mater 51:1841
17. Chen JH, Cao R, Zhang J, Wang GZ (2005) Mater Sci Technol 21(5):507